PERGAMON

International Journal of Solids and Structures 38 (2001) 289–306

INTERNATIONAL JOURNAL OF SOLIDS and STRUCTURES

www.elsevier.com/locate/ijsolstr

A particular integral BEM/time-discontinuous FEM methodology for solving 2-D elastodynamic problems

Chyou-Chi Chien *, Tong-Yue Wu

Department of Civil Engineering, Chung-Yuan University, Chung-Li 32023, Taiwan, ROC

Received 23 March 1999; in revised form 31 August 1999

Abstract

This study proposes a time-discontinuous Galerkin finite element method (FEM) for solving second-order ordinary differential equations in the time domain. The equations are formulated using a particular integral boundary element method (BEM) in the space domain for elastodynamic problems. The particular integral BEM technique depends only on elastostatic displacement and traction fundamental solutions, without resorting to commonly used complex fundamental solutions for elastodynamic problems. Based on the time-discontinuous Galerkin FEM, the unknown displacements and velocities are approximated as piecewise linear functions in the time domain, and are permitted to be discontinuous at the discrete time levels. This leads to stable and third-order accurate solution algorithms for ordinary differential equations. Numerical results using the time-discontinuous Galerkin FEM are compared with results using a conventional finite difference method (the Houbolt method). Both methods are employed for a particular integral BEM analysis in elastodynamics. This comparison reveals that the time-discontinuous Galerkin FEM is more stable and more accurate than the traditional finite difference methods.

Keywords: Particular integral BEM; Time-discontinuous FEM; Elastodynamics; Fundamental solution

1. Introduction

Many numerical techniques have been developed in recent decades to examine the behavior of elastic solids subjected to dynamic loading. The most appropriate methods appear to be the finite element method (FEM) and, more recently, the boundary element method (BEM). These methods have been successfully applied to a wide class of problems in elastodynamics, such as wave propagation, vibration, and soil-structure interaction. The BEM requires discretization of only the *surface* of the domain, but not of its interior, in contrast to *domain* type methods, such as the FEM and the finite difference method. Different boundary element procedures have been presented to deal with elastodynamic problems. Earlier works concentrated on numerically formulating and solving the boundary integral equation in the frequency domain using the Laplace transformation (Cruse, 1968; Cruse and Rizzo, 1968; Shaw, 1979).

* Corresponding author. Tel.: +886-3-4563171, ext. 4209; fax: +886-3-4563171, ext. 4299.
E-mail address: chyouchi@cycu.edu.tw (C.-C. Chien).

0020-7683/00/$ - see front matter
PII: S0020-7683(00)00024-X

In this case, a numerical inverse transformation was required to bring the transformed solution back to the original time domain (Manolis and Beskos, 1981). Niwa et al. (1975, 1976) derived another solution for transient problems using the Fourier transformation and the frequency domain BE formulation. The time domain solutions of the problem were then evaluated using the BEM in conjunction with conventional step-by-step time integration schemes (Cole et al., 1978; Niwa et al., 1980). More recently, Nardini and Brebbia (1982, 1985) developed a more efficient BE formulation (dual reciprocity BEM formulation) for free vibration analysis; later, Ahmad and Banerjee (1986) also derived BEM for free vibration analysis with particular integrals. Herein, the accuracy and efficiency in the solution of realistic engineering problems with the Ahmad and Banerjee method (1986) were superior to the Ahmad and Banerjee method. However, Polyzos et al. (1994) established the equivalence of the dual reciprocity BEM to the particular integral BEM. These two procedures are preferred over previous ones, because the BE equation is cast in the same form as that of dynamic equilibrium equations in finite element analysis. Therefore, the extensive experience in finite element dynamic analysis can be confidently used. Moreover, it is far more straightforward than the time domain BEM formulation, because using a time-independent elastostatic fundamental solution very much simplifies the BEM solution process (Dominguez, 1993). Agnantiaris et al. (1998) recently applied the dual reciprocity BEM to elastodynamic problems in 3-D cases. In their study, the second-order ordinary differential equations or dynamic equilibrium equations, formulated by the dual reciprocity BEM or the particular integral BEM, were solved using traditional step-by-step time integration algorithms. Very recently, the traditional time-domain BEM formulation (Mansur et al., 1998) was employed for scalar wave propagation analysis in which a procedure to consider linear time-discontinuous interpolation for boundary flux was worked out. Such a formulation must use time-dependent fundamental solutions which originated from time and space Dirac delta functions in infinite domains.

Most finite element procedures for the dynamic analysis of continuous models are traditionally based on semidiscretizations: finite elements are used only in space, to reduce the partial differential equations to a system of second-order ordinary differential equations in time. These are the governing equations for discrete models known as the semidiscrete equations of structural dynamics. The semidiscrete equations are further solved by means of the modal superposition method or the step-by-step time integration methods (finite difference discretizations in time). Over the past decades, many efficient algorithms for the step-by-step integration of equations of structural dynamics have been developed. Among these, the second-order accurate and implicit methods, such as the method of Houbolt (1950), the method of Newmark (1959), the Wilson-θ method (Wilson et al., 1973), and the HHT-α method (Hilber et al., 1977), are most frequently used in practice. Many researchers have attempted to use finite elements in the time domain (Argyris and Scharpf, 1969; Fried, 1969; Oden, 1969). Based on Hamilton's principle for dynamics and using *continuous* weighting functions in time, space-time finite element formulations were derived. This often leads to a coupled matrix system in which variables at all time levels must be solved simultaneously. In practice, procedures of this kind have been used rarely, due to their prohibitively high cost. Actually, by multiplying the structural dynamic equations with weighting functions and integrating over time intervals, traditional ordinary differential equation algorithms have been re-derived by Zienkiewicz and Taylor (1991).

Another finite element approach in the time domain is based on a *discontinuous* Galerkin (DG) method. According to this method, the unknown fields are permitted to be discontinuous at the discrete time levels. The DG method has been successfully applied to first-order hyperbolic problems (fluid mechanics) and parabolic problems (transient heat conduction) (Johnson et al., 1984; Johnson, 1987; Thomée, 1984). Hughes and Hulbert (1988) first applied this new approach to the area of structural dynamics. They demonstrated that the DG method possesses considerable potential not present in the traditional semi-discrete methods. In particular, it leads to stable, higher-order accurate solution algorithms to solve ordinary differential equations, and is capable of filtering out the effect of spurious high modes. Very recently,

Li and Wiberg (1996) applied the DG method to 2-D structural dynamic problems. They dealt with the specific DG method that uses piecewise linear interpolations for both displacements and velocities, i.e., the P1–P1 two-field formulation (Hulbert, 1992). This type of element has the advantage over other DG elements with respect to the computational effort needed and its stability and convergence properties (Johnson, 1993; French, 1993).

In this study, 2-D elastodynamic problems are analyzed by BEM using particular integrals in a spatial domain. Since the dynamic equilibrium equation formulated by BEM using particular integrals is similar to that in dynamic FEM analysis, the use of the time-discontinuous Galerkin finite element method is applied to solve dynamic equilibrium equations of the system. Numerical results using the proposed approach and the commonly used Houbolt method (Nardini and Brebbia, 1985) to solve elastodynamic problems are also compared.

2. Boundary element formulation using particular integrals

Consider an elastic solid enclosed by a boundary surface. The equations of motion expressed in terms of the displacement field in the absence of body force are as follows:

$$(\lambda+\mu)u_{j,ij}+\mu u_{i,jj}=\rho\ddot{u}_i, \tag{1}$$

where λ and μ are Lame's constants, ρ is mass density, and $\ddot{u}_i$ are acceleration components. The complementary functions and particular functions are denoted by u_i^{c} and u_i^{p}, respectively. Hence,

$$(\lambda+\mu)u^{\mathrm{c}}_{j,ij}+\mu u^{\mathrm{c}}_{i,jj}=0, \tag{2}$$

$$(\lambda+\mu)u^{\mathrm{p}}_{j,ij}+\mu u^{\mathrm{p}}_{i,jj}=\rho\ddot{u}_i. \tag{3}$$

The acceleration components are represented in the following form:

$$\ddot{u}_i(x)=\sum_{m=1}^{\infty}C_{ik}(x,\xi^m)\Phi_k(\xi^m), \tag{4}$$

where x and ξ^m are the coordinates of field point and source point, respectively, Φ_k is a fictitious density, and C_{ik} is a known function that can be selected as any linear function of spatial coordinates. A simple function for C_{ik} is selected as follows:

$$C_{ik}=(R-r)\delta_{ik}, \tag{5}$$

where R is the largest distance between two points of the solid, r is the distance between x and ξ.

Eq. (4) can also be expressed in the following matrix form:

$$\ddot{\boldsymbol{u}}=\boldsymbol{P}\boldsymbol{\Phi}, \tag{6}$$

or

$$\boldsymbol{\Phi}=\boldsymbol{V}\ddot{\boldsymbol{u}}, \tag{7}$$

where $\boldsymbol{V}=\boldsymbol{P}^{-1}$. By substituting Eq. (4) into Eq. (3), we can choose a particular solution as

$$u_i^{\mathrm{p}}(x)=\sum_{m=1}^{\infty}D_{ik}(x,\xi^m)\Phi_k(\xi^m) \tag{8}$$

in which $D_{ik}(x,\xi^m)$ is a known function in terms of R, r, μ, and ρ indicated in Ahmad and Banerjee (1986).

Eq. (8) can be written in a matrix form as follows:

$$\boldsymbol{u}^{\mathrm{p}} = \boldsymbol{D}\boldsymbol{\Phi}. \tag{9}$$

According to the strain–displacement and the stress–strain relationships, the particular function for the corresponding surface traction is determined by

$$q_i^{\mathrm{p}}(x) = \sum_{m=1}^{\infty} T_{ik}(x, \xi^m)\Phi_k(\xi^m) \tag{10}$$

in which $T_{ik}(x, \xi^m)$ is also a known function in terms of R, r, μ, ρ and n_i indicated in Ahmad and Banerjee (1986).

Eq. (10) can also be written in a matrix form as follows:

$$\boldsymbol{q}^{\mathrm{p}} = \boldsymbol{T}\boldsymbol{\Phi}. \tag{11}$$

By usual discretization of boundary, the corresponding static boundary integral equation of Eq. (2) in a matrix form becomes

$$\boldsymbol{H}\boldsymbol{u}^{\mathrm{c}} = \boldsymbol{G}\boldsymbol{q}^{\mathrm{c}}. \tag{12}$$

Hence, the exact solutions of Eq. (1) becomes

$$\begin{aligned} q_i &= q_i^{\mathrm{c}} + q_i^{\mathrm{p}}, \\ u_i &= u_i^{\mathrm{c}} + u_i^{\mathrm{p}}. \end{aligned} \tag{13}$$

By substituting Eq. (13) into Eq. (12), we obtain

$$\boldsymbol{H}\{\boldsymbol{u} - \boldsymbol{u}^{\mathrm{p}}\} = G\{\boldsymbol{q} - \boldsymbol{q}^{\mathrm{p}}\}. \tag{14}$$

By substituting Eqs. (7), (9) and (11) into Eq. (14), we obtain

$$\{\boldsymbol{G}\boldsymbol{T} - \boldsymbol{H}\boldsymbol{D}\}\boldsymbol{V}\ddot{\boldsymbol{u}} + \tilde{\boldsymbol{H}}\boldsymbol{u} = \tilde{\boldsymbol{G}}\boldsymbol{q} \tag{15}$$

or

$$\tilde{\boldsymbol{M}}\ddot{\boldsymbol{u}} + \tilde{\boldsymbol{H}}\boldsymbol{u} = \tilde{\boldsymbol{G}}\boldsymbol{q}, \tag{16}$$

where the mass matrix $\tilde{\boldsymbol{M}} = \{\boldsymbol{G}\boldsymbol{T} - \boldsymbol{H}\boldsymbol{D}\}\boldsymbol{V}$.

Notably, the pattern of Eq. (16) resembles that of the dynamic equilibrium equation using FEM. To solve Eq. (16), variables of nodal points at the boundary Γ_α, where the displacements are prescribed, are identified by the subscript "α", and the remaining boundary points on Γ_β, by the subscript "β", where the tractions are specified. Hence, Eq. (16) can be rewritten as follows:

$$\tilde{\boldsymbol{M}}_{\alpha\alpha}\ddot{\boldsymbol{u}}_\alpha + \tilde{\boldsymbol{M}}_{\alpha\beta}\ddot{\boldsymbol{u}}_\beta + \tilde{\boldsymbol{H}}_{\alpha\alpha}\boldsymbol{u}_\alpha + \tilde{\boldsymbol{H}}_{\alpha\beta}\boldsymbol{u}_\beta = \tilde{\boldsymbol{G}}_{\alpha\alpha}\boldsymbol{q}_\alpha + \tilde{\boldsymbol{G}}_{\alpha\beta}\boldsymbol{q}_\beta, \tag{17}$$

$$\tilde{\boldsymbol{M}}_{\beta\alpha}\ddot{\boldsymbol{u}}_\alpha + \tilde{\boldsymbol{M}}_{\beta\beta}\ddot{\boldsymbol{u}}_\beta + \tilde{\boldsymbol{H}}_{\beta\alpha}\boldsymbol{u}_\alpha + \tilde{\boldsymbol{H}}_{\beta\beta}\boldsymbol{u}_\beta = \tilde{\boldsymbol{G}}_{\beta\alpha}\boldsymbol{q}_\alpha + \tilde{\boldsymbol{G}}_{\beta\beta}\boldsymbol{q}_\beta. \tag{18}$$

From Eq. (17), $\boldsymbol{q}_\alpha$ can be expressed in the following form:

$$\boldsymbol{q}_\alpha = \tilde{\boldsymbol{G}}_{\alpha\alpha}^{-1}(\tilde{\boldsymbol{M}}_{\alpha\alpha}\ddot{\boldsymbol{u}}_\alpha + \tilde{\boldsymbol{M}}_{\alpha\beta}\ddot{\boldsymbol{u}}_\beta + \tilde{\boldsymbol{H}}_{\alpha\alpha}\boldsymbol{u}_\alpha + \tilde{\boldsymbol{H}}_{\alpha\beta}\boldsymbol{u}_\beta - \tilde{\boldsymbol{G}}_{\alpha\beta}\boldsymbol{q}_\beta). \tag{19}$$

By substituting Eq. (19) into Eq. (18), we can obtain

$$\boldsymbol{M}\ddot{\boldsymbol{u}}_\beta + \boldsymbol{H}\boldsymbol{u}_\beta = \bar{\boldsymbol{M}}\ddot{\boldsymbol{u}}_\alpha + \bar{\boldsymbol{H}}\boldsymbol{u}_\alpha + \hat{\boldsymbol{G}}\boldsymbol{q}_\beta, \tag{20}$$

where

$$\boldsymbol{M} = \tilde{\boldsymbol{M}}_{\beta\beta} - \tilde{\boldsymbol{G}}_{\beta\alpha}\tilde{\boldsymbol{G}}_{\alpha\alpha}^{-1}\tilde{\boldsymbol{M}}_{\alpha\beta},$$

$$\boldsymbol{H} = \tilde{\boldsymbol{H}}_{\beta\beta} - \tilde{\boldsymbol{G}}_{\beta\alpha}\tilde{\boldsymbol{G}}_{\alpha\alpha}^{-1}\tilde{\boldsymbol{G}}_{\alpha\beta},$$

$$\hat{\boldsymbol{G}} = \tilde{\boldsymbol{G}}_{\beta\beta} - \tilde{\boldsymbol{G}}_{\beta\alpha}\tilde{\boldsymbol{G}}_{\alpha\alpha}^{-1}\tilde{\boldsymbol{H}}_{\alpha\beta},$$

$$\bar{\boldsymbol{M}} = \tilde{\boldsymbol{G}}_{\beta\alpha}\tilde{\boldsymbol{G}}_{\alpha\alpha}^{-1}\tilde{\boldsymbol{M}}_{\alpha\alpha} - \tilde{\boldsymbol{M}}_{\beta\alpha},$$

$$\bar{\boldsymbol{H}} = \tilde{\boldsymbol{G}}_{\beta\alpha}\tilde{\boldsymbol{G}}_{\alpha\alpha}^{-1}\tilde{\boldsymbol{H}}_{\alpha\alpha} - \tilde{\boldsymbol{H}}_{\beta\alpha}.$$

On the right-hand side of Eq. (20), all the physical variables are prescribed and we can rewrite Eq. (20) in the compact form (Nardini and Brebbia, 1985)

$$\boldsymbol{M}\ddot{\boldsymbol{u}} + \boldsymbol{H}\boldsymbol{u} = \boldsymbol{F}, \tag{21}$$

where $\boldsymbol{M}$ is the equivalent *mass* matrix, $\boldsymbol{H}$ is the equivalent *stiffness* matrix, and $\boldsymbol{F}$ is the equivalent *load* vector. The known boundary conditions are given by

$$u_i(x,t) = \bar{u}_i(x,t), \;\; x \in \Gamma_\alpha \quad \text{and} \quad q(x,t) = \bar{q}_i(x,t), \;\; x \in \Gamma_\beta \tag{22}$$

with $\Gamma_\alpha \cup \Gamma_\beta = \Gamma$, $\Gamma_\alpha \cap \Gamma_\beta = \phi$, where $\bar{u}_i$ is the prescribed displacements on Γ_α and $\bar{q}_i$ are the prescribed tractions on Γ_β. Meanwhile, the initial conditions are given by

$$u_i(x,0) = u_0(x), \;\; x \in \Omega \quad \text{and} \quad \dot{u}_i(x,0) = v_0(x), \;\; x \in \Omega, \tag{23}$$

where x is in the domain of the solid.

Once the previous boundary and initial conditions are introduced, the system of equation (21) can be solved using any one of the existing step-by-step time integration approaches, such as the Houbolt method, the Newmark method, the Wilson-θ method, or the HHT-α method. This study employs a time finite element approach or a time-discontinuous Galerkin method, which uses piecewise linear interpolation functions for both displacements and velocities. It is worth pointing out that the influence matrices $\boldsymbol{H}$ and $\boldsymbol{G}$ in Eq. (12) contain the evaluations of strong- and weak-singular integrals, respectively, which are the same as those of the elastostatic fundamental solutions (Brebbia et al., 1984; Banerjee, 1994).

3. Time-discontinuous Galerkin finite element formulation

Eqs. (21) and (23) can be rewritten in the compact form:

$$\begin{aligned} \boldsymbol{M}\dot{\boldsymbol{v}} + \boldsymbol{H}\boldsymbol{u} - \boldsymbol{F} &= 0, \\ \boldsymbol{H}(\dot{\boldsymbol{u}} - \boldsymbol{v}) &= 0. \end{aligned} \tag{24}$$

Consider a partition of the time domain, $I = (0,T)$, having the form: $0 = t_1 < t_2 < \cdots < t_n < t_{n+1} < \cdots < t_{N+1} = T$. Let the time steps $\Delta t_n = t_{n+1} - t_n$ and $I_n = (t_n, t_{n+1})$. Make the following specific choice of the time finite element space:

$$\boldsymbol{V}^h = \left\{ \boldsymbol{w}^h \in \bigcup_{n=1}^{N} \left(\boldsymbol{P}^1(\boldsymbol{I}_n)\right)^{n_{\text{eq}}} \right\}, \tag{25}$$

where $\boldsymbol{P}^1$ denotes the first-order polynomial, and each member of $\boldsymbol{V}^h$ is a vector consisting of n_{eq} linear functions on each time step I_n. All trial displacements and velocities and their corresponding weighting functions are chosen from the space $\boldsymbol{V}^h$. Notably, the functions in $\boldsymbol{V}^h$ may be discontinuous at the discrete time levels t_n. To account for this, we introduce the notation,

$$w_n^+ = \lim_{\varepsilon \to 0^+} w(t_n + \varepsilon), \tag{26}$$

$$w_n^- = \lim_{\varepsilon \to 0^-} w(t_n + \varepsilon). \tag{27}$$

Note that the functions are continuous over each time interval but allow *jumps* at the discrete time levels t_n. The weak formulation of the time-discontinuous Galerkin finite element in a typical time step $I_n = (t_n, t_{n+1})$ with respect to Eq. (24) can be expressed as follows:

Find $\boldsymbol{U}^h = \{\boldsymbol{u}^h, \boldsymbol{v}^h\} \in \boldsymbol{V}^h \times \boldsymbol{V}^h$ such that for all $\boldsymbol{W}^h = \{\boldsymbol{w}_1^h, \boldsymbol{w}_2^h\} \in \boldsymbol{V}^h \times \boldsymbol{V}^h$, and let

$$\boldsymbol{R}_n = \int_{I_n} \boldsymbol{w}_2^h (\mathsf{L}_1 \boldsymbol{U}^h - \boldsymbol{F})\,\mathrm{d}t + \int_{I_n} \boldsymbol{w}_1^h \cdot \boldsymbol{H} \mathsf{L}_2 \boldsymbol{U}^h\,\mathrm{d}t + \boldsymbol{w}_1^h(t_n^+) \cdot \boldsymbol{H}\left[\boldsymbol{u}^h(t_n)\right] + \boldsymbol{w}_2^h(t_n^+) \cdot \boldsymbol{M}\left[v^h(t_n)\right] = 0,$$
$$n = 1, \ldots, N, \tag{28}$$

where

$$\mathsf{L}_1 \boldsymbol{U}^h = \boldsymbol{M}\dot{\boldsymbol{v}}^h + \boldsymbol{H}\boldsymbol{u}^h, \tag{29}$$

$$\mathsf{L}_2 \boldsymbol{U}^h = \dot{\boldsymbol{u}}^h - \boldsymbol{v}^h. \tag{30}$$

It has been shown that the above time-discontinuous Galerkin finite element method using the P1–P1 two-field formulation element is unconditionally stable and of third-order accuracy (Hulbert, 1992, 1994).

In the following, we present an iterative solution algorithm to obtain the solutions for the resulting system of equations from Eq. (28). Considering a typical time step $I_n = (t_n, t_{n+1})$, let $\boldsymbol{u}_1$ and $\boldsymbol{v}_1$ denote the nodal displacements and velocities at t_n^+, respectively, and $\boldsymbol{u}_2$ and $\boldsymbol{v}_2$ the nodal displacements and velocities at t_{n+1}^-, respectively. Also, let $\boldsymbol{u}_1^-$ and $\boldsymbol{v}_1^-$ represent the nodal displacements and velocities at t_n^-, respectively, which are determined from either the previous step's calculations or, if $n = 1$, the initial data. Thus, the displacements and velocities at an arbitrary time $t \in (t_n, t_{n+1})$ can be expressed as follows:

$$\boldsymbol{u}^h(t) = \phi_1(t)\boldsymbol{u}_1 + \phi_2(t)\boldsymbol{u}_2, \tag{31a}$$

$$\boldsymbol{v}^h(t) = \phi_1(t)\boldsymbol{v}_1 + \phi_2(t)\boldsymbol{v}_2, \tag{31b}$$

where $\phi_1(t) = (t_{n+1} - t)/\Delta t_n$ and $\phi_2(t) = (t - t_n)/\Delta t_n$, i.e., the P1–P1 element is defined for the displacement and velocity fields (Hulbert, 1992, 1994). By substituting Eq. (31) and their corresponding weighting functions into Eq. (28), and performing the integration explicitly, one can obtain the following matrix equation as follows:

$$\begin{bmatrix} \frac{1}{2}\boldsymbol{H} & \frac{1}{2}\boldsymbol{H} & -\frac{1}{3}\Delta t_n \boldsymbol{H} & -\frac{1}{6}\Delta t_n \boldsymbol{H} \\ -\frac{1}{2}\boldsymbol{H} & \frac{1}{2}\boldsymbol{H} & -\frac{1}{6}\Delta t_n \boldsymbol{H} & -\frac{1}{3}\Delta t_n \boldsymbol{H} \\ \frac{1}{3}\Delta t_n \boldsymbol{H} & \frac{1}{6}\Delta t_n \boldsymbol{H} & \frac{1}{2}\boldsymbol{M} & \frac{1}{2}\boldsymbol{M} \\ \frac{1}{6}\Delta t_n \boldsymbol{H} & \frac{1}{3}\Delta t_n \boldsymbol{H} & -\frac{1}{2}\boldsymbol{M} & \frac{1}{2}\boldsymbol{M} \end{bmatrix} \begin{Bmatrix} \boldsymbol{u}_1 \\ \boldsymbol{u}_2 \\ \boldsymbol{v}_1 \\ \boldsymbol{v}_2 \end{Bmatrix} = \begin{Bmatrix} \boldsymbol{H}\boldsymbol{u}_1^- \\ 0 \\ \boldsymbol{F}_1 + \boldsymbol{M}\boldsymbol{v}_1^- \\ \boldsymbol{F}_2 \end{Bmatrix}, \tag{32}$$

where

$$\boldsymbol{F}_1 = \int_{I_n} \phi_1(t)\boldsymbol{F}\,\mathrm{d}t, \qquad \boldsymbol{F}_2 = \int_{I_n} \phi_2(t)\boldsymbol{F}\,\mathrm{d}t. \tag{33}$$

Solving Eq. (32) is a non-trivial task, because this equation is coupled and four times larger than the original equation (21). An iterative predictor/multi-corrector algorithm is designed to decrease the computational cost (Li and Wiberg, 1996). We first recast the system as follows:

$$\begin{bmatrix} \boldsymbol{H} & 0 & -\frac{1}{6}\Delta t_n \boldsymbol{H} & \frac{1}{6}\Delta t_n \boldsymbol{H} \\ 0 & \boldsymbol{H} & -\frac{1}{2}\Delta t_n \boldsymbol{H} & -\frac{1}{2}\Delta t_n \boldsymbol{H} \\ 0 & 0 & \boldsymbol{M}^* & \frac{2}{3}\boldsymbol{M} \\ 0 & 0 & \frac{1}{3}\Delta t_n^2 \boldsymbol{H} & \boldsymbol{M}^* \end{bmatrix} \begin{Bmatrix} \boldsymbol{u}_1 \\ \boldsymbol{u}_2 \\ \boldsymbol{v}_1 \\ \boldsymbol{v}_2 \end{Bmatrix} = \begin{Bmatrix} \boldsymbol{H}\boldsymbol{u}_1^- \\ \boldsymbol{H}\boldsymbol{u}_2^- \\ \boldsymbol{F}_1^* \\ \boldsymbol{F}_2^* \end{Bmatrix}, \tag{34}$$

where

$$\boldsymbol{M}^* = \boldsymbol{M} + \tfrac{1}{6}\Delta t_n^2 \boldsymbol{H}, \tag{35}$$

$$\boldsymbol{F}_1^* = \tfrac{5}{3}\left(\boldsymbol{F}_1 + \boldsymbol{M}\boldsymbol{v}_1^-\right) - \tfrac{1}{3}\boldsymbol{F}_2 - \tfrac{2}{3}\Delta t_n \boldsymbol{H}\boldsymbol{u}_1^-, \tag{36}$$

$$\boldsymbol{F}_2^* = \boldsymbol{F}_1 + \boldsymbol{F}_2 + \boldsymbol{M}\boldsymbol{v}_1^- - \Delta t_n \boldsymbol{H}\boldsymbol{u}_1^- \tag{37}$$

are the effective mass matrix and force vectors. Clearly, the third and fourth rows in Eq. (32) have been partially decoupled from the first and second ones, and they can be solved separately as follows:

$$\begin{bmatrix} \boldsymbol{M}^* & \frac{2}{3}\boldsymbol{M} \\ \frac{1}{3}\Delta t_n^2 \boldsymbol{H} & \boldsymbol{M}^* \end{bmatrix} \begin{Bmatrix} \boldsymbol{v}_1 \\ \boldsymbol{v}_2 \end{Bmatrix} = \begin{Bmatrix} \boldsymbol{F}_1^* \\ \boldsymbol{F}_2^* \end{Bmatrix}. \tag{38}$$

If initial predictor values of $\boldsymbol{v}_1$ and $\boldsymbol{v}_2$ are given, for instance, the chosen being v_1^-, Eq. (38) is solved iteratively for the corrected values of $\boldsymbol{v}_1$ and $\boldsymbol{v}_2$, until the required accuracy is obtained. In the numerical examples, an accuracy requirement of $\varepsilon = 10^{-6}$ is specified, and the iteration process is performed until $\varepsilon = \|(\boldsymbol{v}_1^{k+1} - \boldsymbol{v}_1^k), (\boldsymbol{v}_2^{k+1} - \boldsymbol{v}_2^k)\|$ is met. Then, the first row in Eq. (34) is used for determining $\boldsymbol{u}_1$ and the second one for determining $\boldsymbol{u}_2$. The above solution algorithm is summarized in Table 1, which demonstrates that the implementation of the DG method is not complex. Notably, this table adopts the accelerated Gauss–Seidel iteration scheme with the factor of acceleration ω, which is known as the successive over-relaxation (or SOR) method. The SOR method can effectively reduce the iterative time of the computation when solving the linear system of equations. This procedure is superior to that described in the article by Li and Wiberg (1996) (using the Gauss–Jacobi iteration method).

4. Numerical examples

Three numerical examples concerning the transient responses of 2-D elastic bodies are presented. In this study, three-noded quadratic elements are employed for the BEM in the space domain, and two-noded linear elements are adopted for the FEM in the time domain. The traction discontinuity at the corner is modeled through the use of double nodes. One is refered to Brebbia et al. (1984) or Banerjee (1994) for further details regarding numerical implementation. In order to improve the accuracy, internal points can be introduced in the BEM formulation (Nardini and Brebbia, 1982). Numerical results are compared with those obtained by other numerical methods (the Houbolt method or FEM) and/or with exact solutions, to assess the stability and the accuracy of the proposed method.

Example 1. The first problem in this example concerns a rectangular plate subjected to an end tensile traction of a time-dependent Heaviside type as depicted in Fig. 1(a) and (b). The material properties are Poisson's ratio $v = 0$, shear modulus $\mu = 40$ kPa, and mass density $\rho = 1.0$ kg/m^3. The boundary element discretization consists of 12 elements, and five internal points are uniformly distributed in the space domain. The time histories of the vertical displacement at point A are obtained and compared with the

Table 1
Solution algorithm of the DG method

a. Data input and initialization:

$\boldsymbol{u}_1^- = \boldsymbol{u}_0$
$\boldsymbol{v}_1^- = \boldsymbol{v}_0$
$t = 0$

b. Form effective mass matrix and perform factorization:

$\boldsymbol{M}^* = \boldsymbol{M} + \frac{1}{6}\Delta t^2 \boldsymbol{H}$

c. Time integration:

(1) Form generalized force vectors:

$\boldsymbol{F}_1^* = \frac{1}{3}\left(5\boldsymbol{F}_1 + 5\boldsymbol{M}\boldsymbol{v}_1^- - \boldsymbol{F}_2 - 2\Delta t \boldsymbol{H}\boldsymbol{u}_1^-\right)$
$\boldsymbol{F}_2^* = \boldsymbol{F}_1 + \boldsymbol{F}_2 + \boldsymbol{M}\boldsymbol{v}_1^- - \Delta t \boldsymbol{H}\boldsymbol{u}_1^-$

(2) Predictor:

$\boldsymbol{v}_1 = \boldsymbol{v}_1^-$
$\boldsymbol{v}_2 = \boldsymbol{v}_2^-$
$i = 0$

(3) Multi-corrector:

$\boldsymbol{M}^* \boldsymbol{v}_1^{(i+1)} = \omega\left[\boldsymbol{F}_1^* - \left(\frac{2}{3}\boldsymbol{M}\right)\boldsymbol{v}_2^{(i)}\right]$
$\boldsymbol{v}_1^{(i+1)} = \boldsymbol{v}_1^{(i+1)} + (1-\omega)\boldsymbol{v}_1^{(i)}$
$\boldsymbol{M}^* \boldsymbol{v}_2^{(i+1)} = \omega\left[\boldsymbol{F}_2^* - \left(\frac{1}{3}\Delta t^2 \boldsymbol{H}\right)\boldsymbol{v}_1^{(i)}\right]$
$\boldsymbol{v}_2^{(i+1)} = \boldsymbol{v}_2^{(i+1)} + (1-\omega)\boldsymbol{v}_2^{(i)}$
$i = i + 1$
If $\bar{\varepsilon} > \varepsilon$ go to (3)

(4) Output solution:
$\boldsymbol{v}_1^- \leftarrow \boldsymbol{v}_2$
$\boldsymbol{u}_1^- \leftarrow \boldsymbol{u}_1^- + \frac{\Delta t}{2}(\boldsymbol{v}_1 + \boldsymbol{v}_2)$
$t \leftarrow t + \Delta t$
If $t < T$ go to (1), else stop

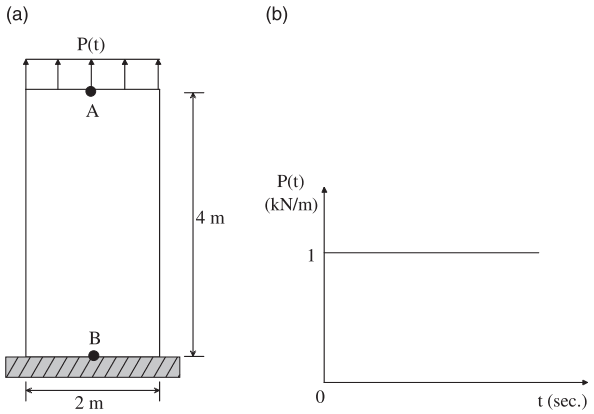

Fig. 1. (a) A rectangular plate subjected to an end tensile traction and (b) the time history of a Heaviside-type traction.

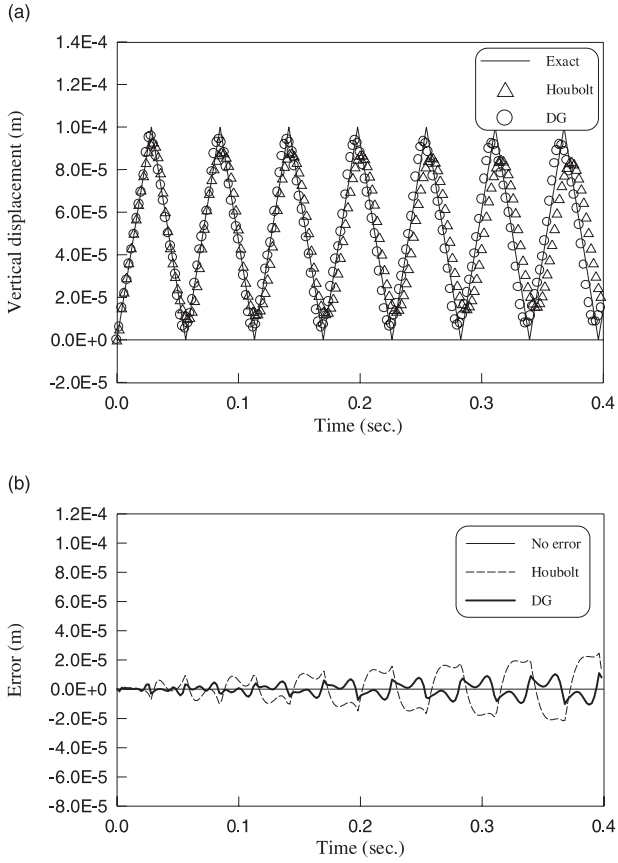

Fig. 2. (a) Vertical displacement and (b) error distribution, at point A of a rectangular plate under a tensile traction with $\beta = 1.0$.

exact solution and the solution using the Houbolt method. Also, the time histories of the error distributions in the numerical solution, i.e., DG or Houbolt solution – exact solution, are obtained. The results for three different step sizes $\beta = 1.0,\ 1.5$ and 2.0 (i.e., $\beta = C_P \Delta t/L$, where C_P is the P-wave velocity, Δt, the time step, and, L, the distance between the nearest nodes) are displayed in Figs. 2–4, respectively. According to these figures, the DG method provides much more accurate solutions than the Houbolt method. Specifically, the Houbolt method introduces more amplitude decay and period elongation than the DG method. Notably, a very accurate solution can be obtained by the DG method with a fairly big step size, a result which the Houbolt method cannot achieve. The time histories of axial stress at point B presented in Figs. 5–7 further prove that the DG method provides better results than the Houbolt method.

Example 2. The second problem in this example concerns a rectangular plate subjected to an end tensile traction of a triangular time variation, as depicted in Fig. 8(a) and (b). The material properties are Poisson's ratio $v = 0$, shear modulus $\mu = 40$ kPa, and mass density $\rho = 1.0$ kg/m^3. The boundary element discretization consists of 24 elements, and 10 internal points are uniformly distributed in the domain. The time histories of the vertical displacement at point A are obtained and compared with the exact solution

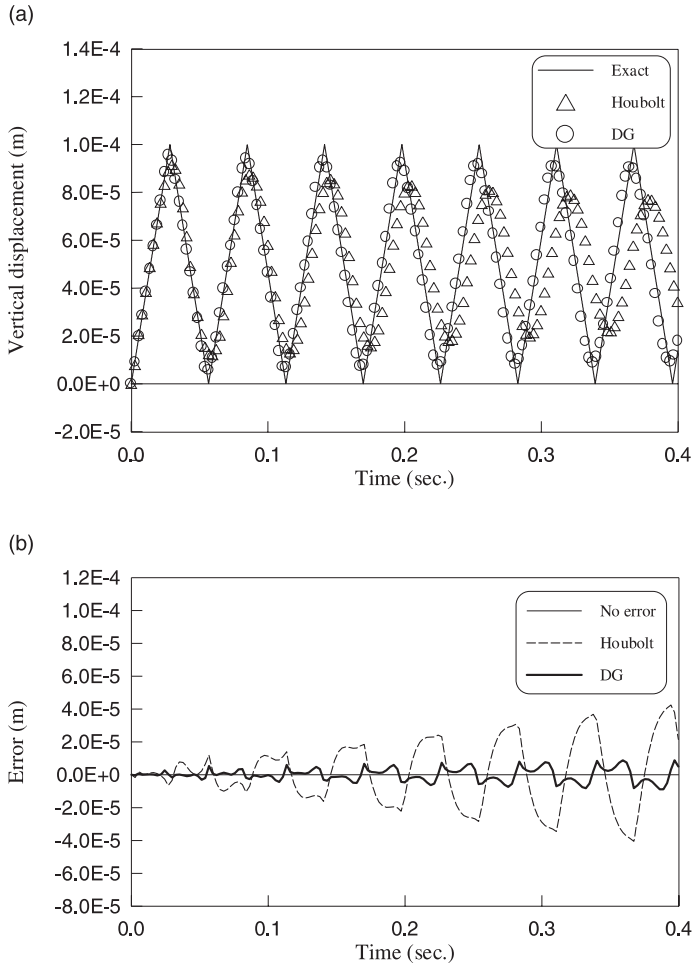

Fig. 3. (a) Vertical displacement and (b) error distribution, at point A of a rectangular plate under a tensile traction with $\beta = 1.5$.

and the solution using the Houbolt method. The time histories of the error distributions in the numerical solution, i.e., DG or Houbolt solution – exact solution, are obtained. The results for three different step sizes $\beta = 1.0$, 1.5 and 2.0 are displayed in Figs. 9–11, respectively. In addition, the time histories of axial stress at point B are presented in Figs. 12–14. According to these figures, the DG method still offers much more accurate solutions than the Houbolt method. It is observed that, even with big step sizes compared with the Houbolt method, the DG method follows the exact solution fairly well as obtained in Example 1.

Example 3. In the final example, a rectangular plate is subjected to an end flexural traction of a triangular time variation, as depicted in Fig. 15(a) and (b). The material properties are Poisson's ratio $v = 0.3$, shear modulus $\mu = 40$ kPa, and mass density $\rho = 1.0$ kg/m^3. The boundary element model is the same as that of Example 1, and five internal points are also employed in the analysis. The exact solution for such a problem is unavailable and hence the DG solution for the time histories of horizontal displacement at

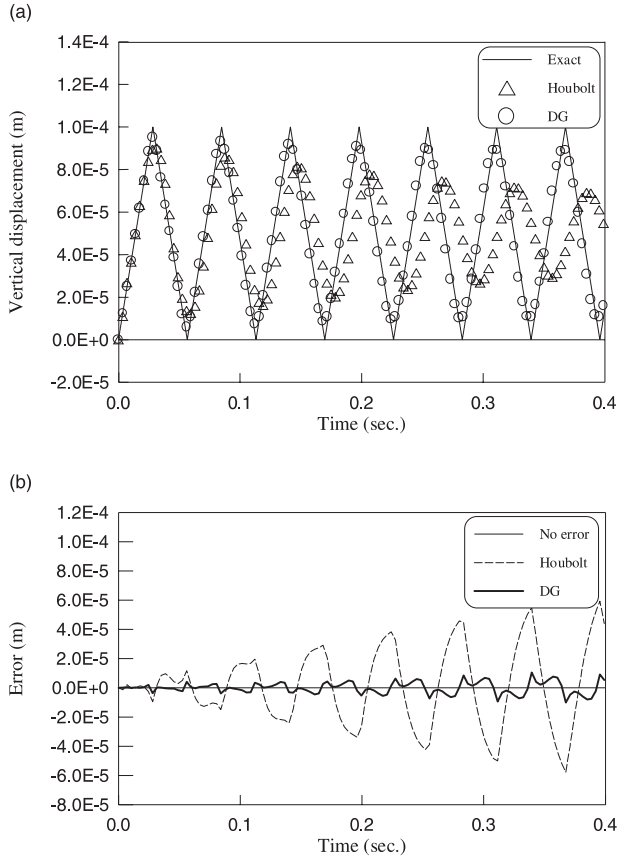

Fig. 4. (a) Vertical displacement and (b) error distribution, at point A of a rectangular plate under a tensile traction with $\beta = 2.0$.

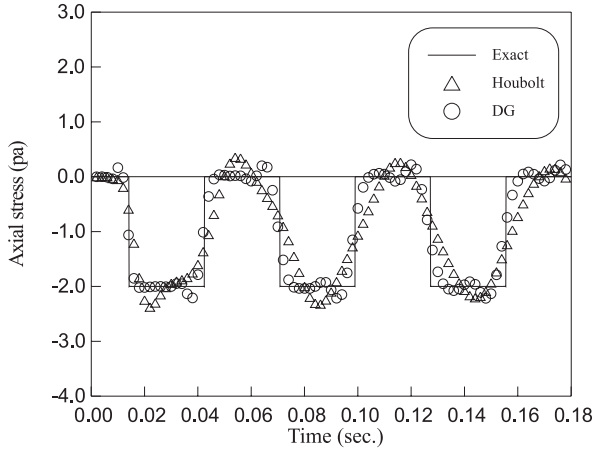

Fig. 5. Axial stress at point B of a rectangular plate under a tensile traction with $\beta = 1.0$.

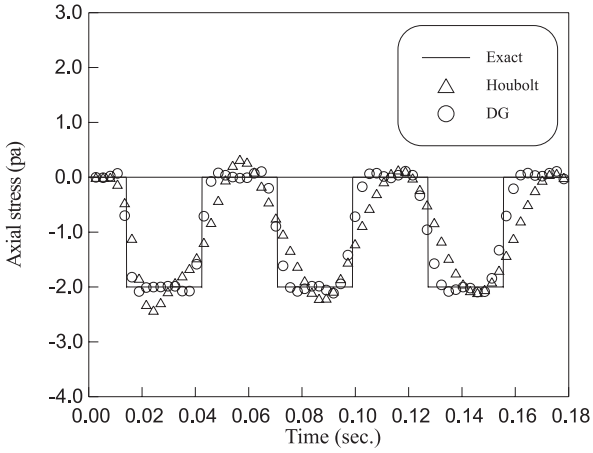

Fig. 6. Axial stress at point B of a rectangular plate under a tensile traction with $\beta = 1.5$.

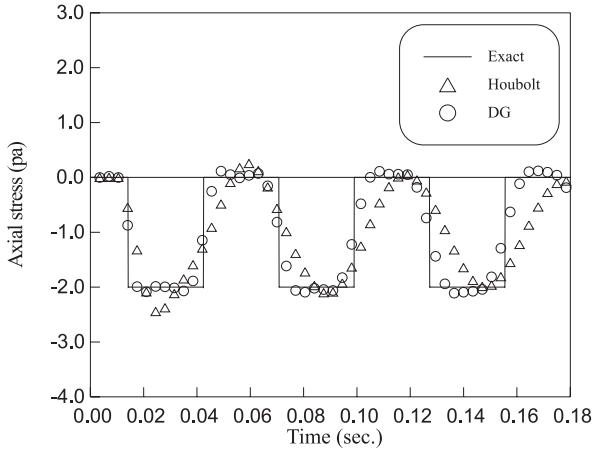

Fig. 7. Axial stress at point B of a rectangular plate under a tensile traction with $\beta = 2.0$.

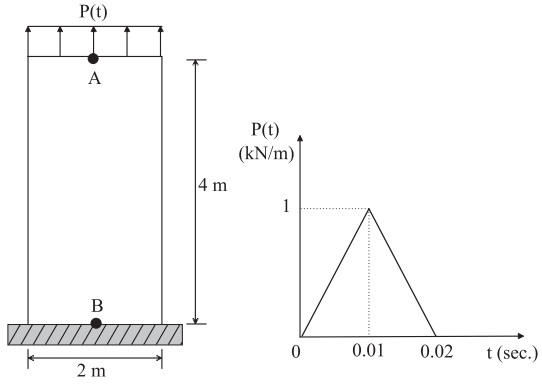

Fig. 8. (a) A rectangular plate subjected to an end tensile traction and (b) the time history of a triangular time variation traction.

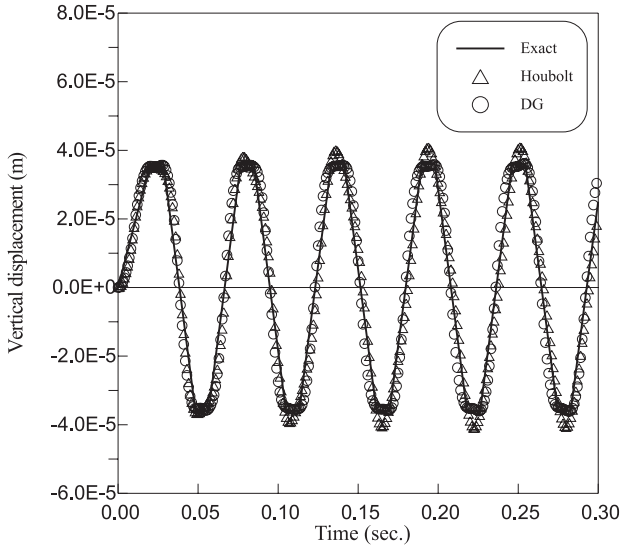

Fig. 9. Vertical displacement at point A of a rectangular plate under a triangular time variation traction with $\beta = 1.0$.

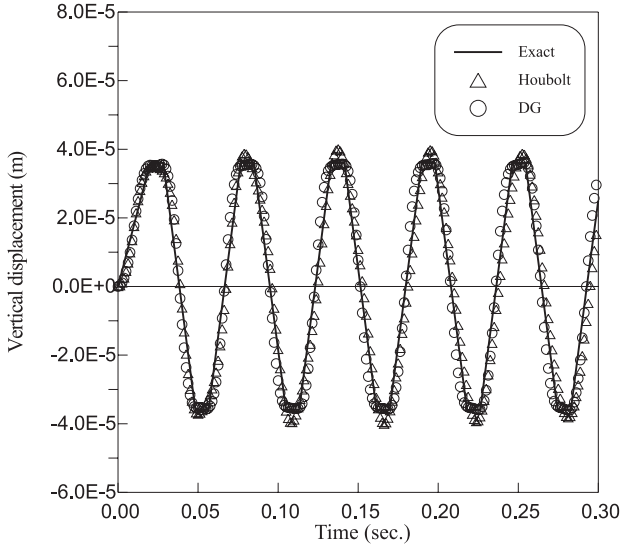

Fig. 10. Vertical displacement at point A of a rectangular plate under a triangular time variation traction with $\beta = 1.5$.

point A is compared with the FEM solution and the Houbolt method. The results for three different step size $\beta = 1.0$, 1.5 and 2.0 are displayed in Figs. 16–18, respectively. The differences between the results from the DG and the Houbolt methods are found to be small. However, the results of the DG method more accurately approach the FEM solution than the Houbolt method, at three peaks of the displacement curve.

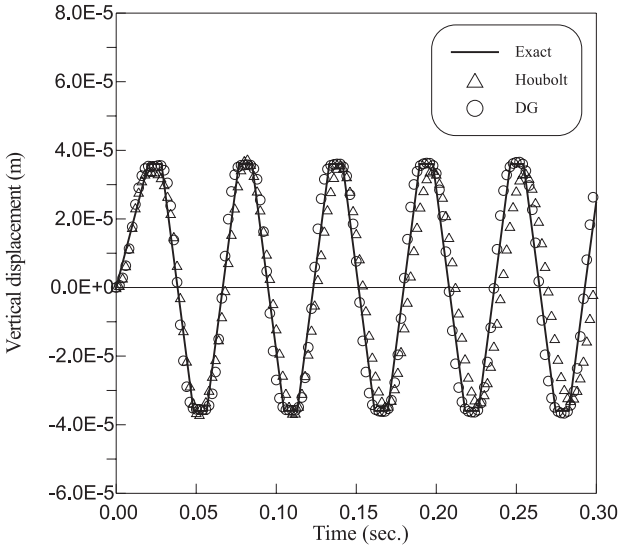

Fig. 11. Vertical displacement at point A of a rectangular plate under a triangular time variation traction with $\beta = 2.0$.

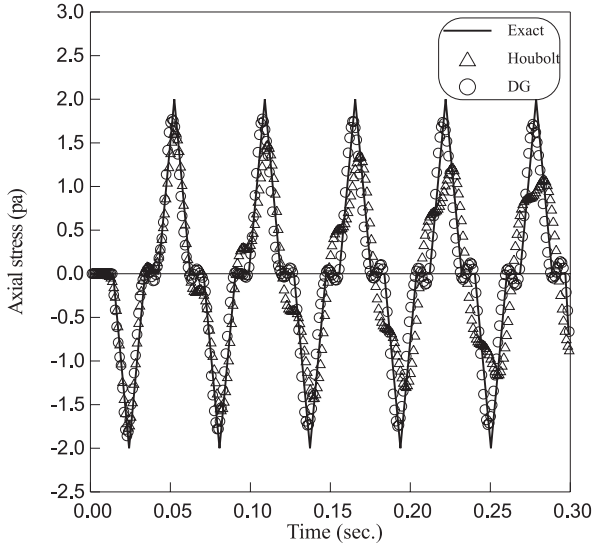

Fig. 12. Axial stress at point B of a rectangular plate under a triangular time variation traction with $\beta = 1.0$.

5. Conclusions

The BEM using particular integrals is presented to analyze the transient problems of two-dimensional elastic solids. By utilizing the particular solutions of the governing differential equation, a surface-only integral equation is derived, and only the elastostatic fundamental solution is used rather than a frequency

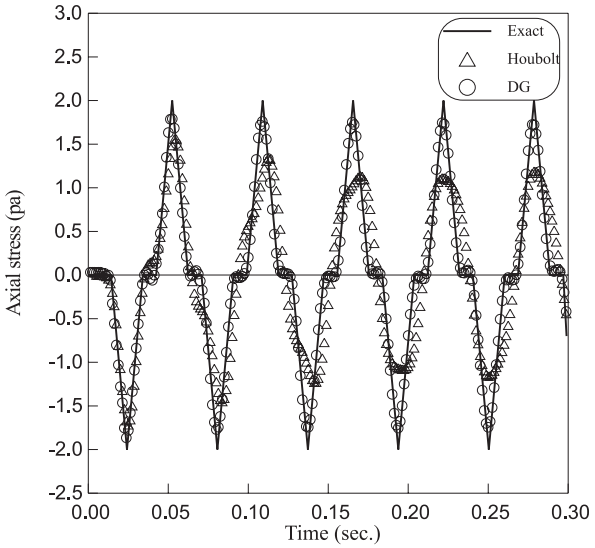

Fig. 13. Axial stress at point B of a rectangular plate under a triangular time variation traction with $\beta = 1.5$.

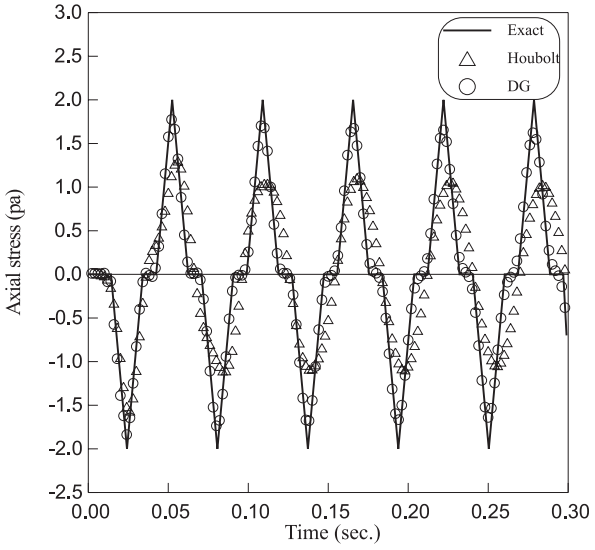

Fig. 14. Axial stress at point B of a rectangular plate under a triangular time variation traction with $\beta = 2.0$.

or time-dependent fundamental solution. Since the resulting system matrix resembles the corresponding FEM matrix, extensive experience in finite element dynamic analysis can be confidently employed. The BEM system matrix in the time domain is solved using a time-discontinuous Galerkin FEM. The numerical examples presented indicate the applicability of these BEM techniques for the solution of elastodynamic problems. Numerical results further indicate that the solution technique based on a discontinuous time finite element procedure is computationally more stable and more accurate than the solution procedure

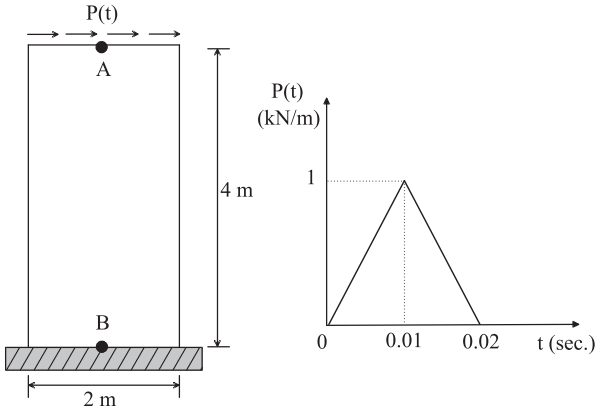

Fig. 15. (a) A rectangular plate subjected to an end flexural traction and (b) the time history of a triangular time variation traction.

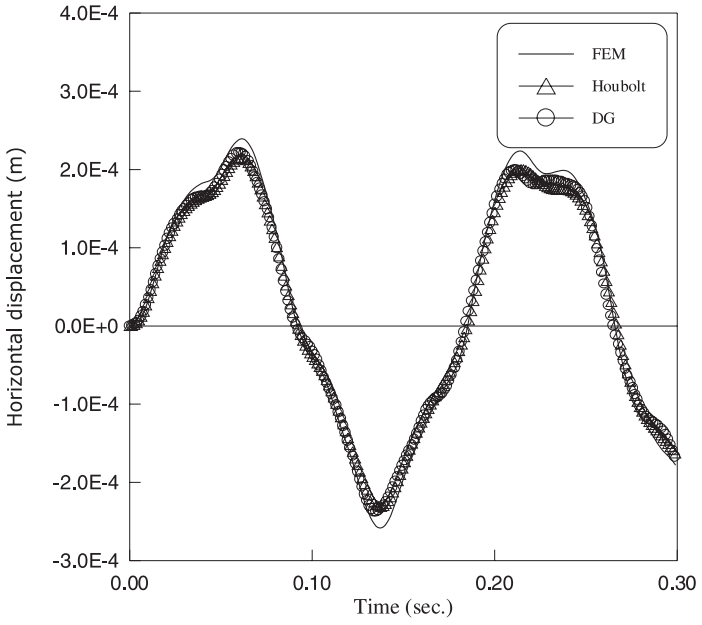

Fig. 16. Horizontal displacement at point A of a rectangular plate under a flexural traction with $\beta = 1.0$.

based on the commonly used Houbolt step-by-step time integration algorithm. The present analysis can be easily extended to 3-D problems involving time-dependent or dynamic responses.

Acknowledgements

The authors would like to thank the National Science Council of the Republic of China for financially supporting this research under Contract No. NSC 88-2211-E-033-003.

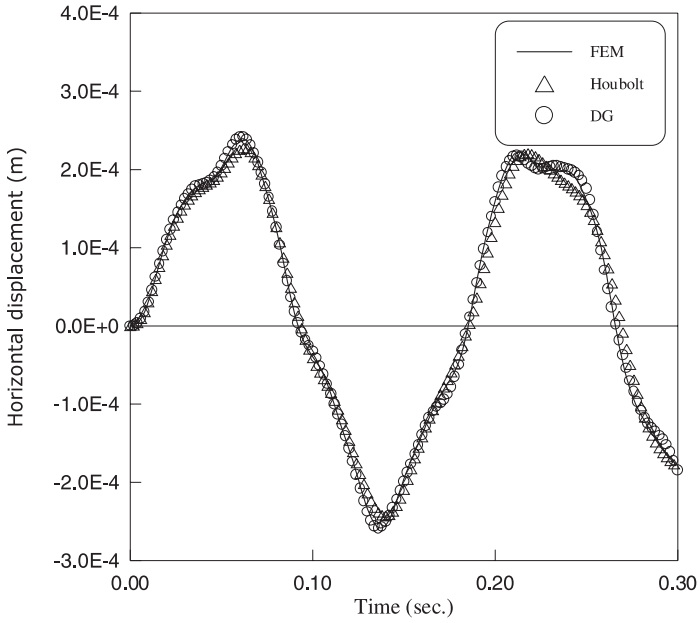

Fig. 17. Horizontal displacement at point A of a rectangular plate under a flexural traction with $\beta = 1.5$.

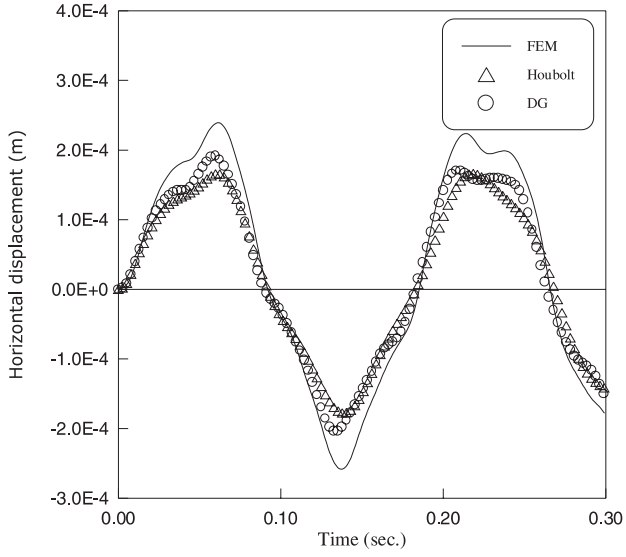

Fig. 18. Horizontal displacement at point A of a rectangular plate under a flexural traction with $\beta = 2.0$.

References

Agnantiaris, J., Polyzos, D., Beskos, D.E., 1998. Three-dimensional structural vibration analysis by dual reciprocity BEM. Comput. Mech. 21, 372–381.

Ahmad, S., Banerjee, P.K., 1986. Free vibration analysis by BEM using particular integrals. J. Engng. Mech. Div. ASCE 112, 682–695.

Argyris, J., Scharpf, D.W., 1969. Finite elements in time and space. Nucl. Engng. Design 10, 456–464.
Banerjee, P.K., 1994. The Boundary Element Methods in Engineering. McGraw-Hill, London.
Brebbia, C.A., Telles, J.C.F., Wroble, L.C., 1984. Boundary Element Techniques. Springer, Berlin.
Cole, D.M., Kosloff, D.D., Minster, J.B., 1978. A numerical boundary integral equation method for elastodynamics-I. Bull. Seism. Soc. Am. 68 (5), 1331–1357.
Cruse, T.A., 1968. A direct formulation and numerical solution of the general transient elastodynamic problem-II. J. Math. Anal. Applic. 22, 341–355.
Cruse, T.A., Rizzo, F.J., 1968. A direct formulation and numerical solution for the general transient elastodynamic problem-I. J. Math. Anal. Applic. 22, 244–259.
Dominguez, J., 1993. Boundary Elements in Dynamics. Elsevier, Amsterdam.
French, D.A., 1993. A space-time finite element method for the wave equation. Comput. Meth. Appl. Mech. Engng. 107, 145–157.
Fried, I., 1969. Finite element analysis of time-dependent phenomena. AIAA J. 7, 1170–1173.
Hilber, H.M., Hughes, T.J.R., Taylor, R.L., 1977. Improved numerical dissipation for time integration algorithms in structural dynamics. Earthquake Engng. Struct. Dyn. 5, 283–292.
Houbolt, J.C., 1950. A recurrence matrix solution for the dynamic response of elastic aircraft. J. Aeronaut. Sci. 17, 540–550.
Hughes, T.J.R., Hulbert, G., 1988. Space-time finite element methods for elastodynamics: formulation and error estimates. Comput. Meth. Appl. Mech. Engng. 66, 363–393.
Hulbert, G., 1992. Time finite element methods for structural dynamics. Int. J. Num. Meth. Engng. 33, 307–331.
Hulbert, G., 1994. A unified set of single-step asymptotic annihilation algorithms for structural dynamics. Comput. Meth. Appl. Mech. Engng. 113, 1–9.
Johnson, C., Nävert, U., Pitkaranta, J., 1984. Finite element methods for linear hyperbolic problem. Comput. Meth. Appl. Mech. Engng. 45, 285–312.
Johnson, C., 1987. Numerical Solutions of Partial Differential Equations by the Finite Element Method. Cambridge Univ. Press, Cambridge, MA.
Johnson, C., 1993. Discontinuous Galerkin finite element methods for second order hyperbolic problem. Comput. Meth. Appl. Mech. Engng. 107, 117–129.
Li, X.D., Wiberg, N.-E., 1996. Structural dynamic analysis by a time-discontinuous Galerkin finite element method. Int. J. Num. Meth. Engng. 39, 2131–2152.
Manolis, G.D., Beskos, D.E., 1981. Dynamic stress concentration studies by boundary integral and Laplace transformation. Int. J. Num. Meth. Engng. 17, 573–599.
Mansur, W.J., Carrer, J.A.M., Siqueira, E.F.N., 1998. Time discontinuous linear traction approximation in time-domain BEM scalar wave propagation analysis. Int. J. Num. Meth. Engng. 42, 667–683.
Nardini, D., Brebbia, C.A., 1982. A new approach to free vibration analysis using boundary elements. In: Brebbia, C.A. (Ed.), Boundary Element Methods in Engineering. Springer, Berlin, pp. 312–326.
Nardini, D., Brebbia, C.A., 1985. Boundary integral formulation of mass matrices for dynamic analysis. In: Brebbia, C.A. (Ed.), Topics in Boundary Element Research, vol. 2. Springer, Berlin, pp. 191–208.
Newmark, N.M., 1959. A method of computation for structural dynamics. J. Engng. Mech. Div. ASCE 85, 67–94.
Niwa, Y., Kobayashi, S., Azuma, N., 1975. An analysis of transient stress produced around cavities of arbitrary shape during the passage of travelling waves. Mem. Fac. Engng. 37, 28–46.
Niwa, Y., Kobayashi, S., Fukui, T., 1976. Applications of integral equation method to some geomechanical problems. In: Desai, C.S. (Ed.), Numerical Methods in Geomechanics. ASCE, New York, pp. 120–131.
Niwa, Y., Fukui, T., Kato, S., Fujiki, K., 1980. An application of the integral equation method to two-dimensional elastodynamics. Theor. Appl. Mech. 28, 281–290.
Oden, J.T., 1969. A general theory of finite elements II, applications. Int. J. Num. Meth. Engng. 1, 247–259.
Polyzos, D., Dassios, G., Beskos, D.E., 1994. On the equivalence of dual reciprocity and particular integrals approaches in the BEM. Boundary Elem. Commum. 5, 285–288.
Shaw, R.P., 1979. Boundary integral equation methods applied to wave problems. In: Banerjee, P.K., Butterfield, R. (Eds.), Developments in Boundary Element Method, vol. 1. Applied Science Publ., London, pp. 121–153.
Thomée, V., 1984. Galerkin Finite Element Methods for Parabolic Problems. Springer, New York.
Wilson, E.L., Farhoomand, I., Bathe, K.J., 1973. Nonlinear dynamic analysis of complex structures. Earthquake Engng. Struct. Dyn. 1, 241–252.
Zienkiewicz, O.C., Taylor, R.L., 1991. The Finite Element Method, II, Solid and Fluid Mechanics, Dynamics and Nonlinearity. McGraw-Hill, New York.